

# Robust Multi-Robot Coverage of Unknown Environments using a Distributed Robot Swarm

Vu Phi Tran, Matthew A. Garratt, Kathryn Kasmarik, Sreenatha G. Anavatti

**Abstract**—In mobile robotics, area exploration and coverage are critical capabilities. In most of the available research, a common assumption is global, long-range communication and centralised cooperation. This paper proposes a novel swarm-based coverage control algorithm that relaxes these assumptions. The algorithm combines two elements: swarm rules and frontier search algorithms. Inspired by natural systems in which large numbers of simple agents (e.g., schooling fish, flocking birds, swarming insects) perform complicated collective behaviors, the first element uses three simple rules to maintain a swarm formation in a distributed manner. The second element provides means to select promising regions to explore (and cover) using the minimization of a cost function involving the agent's relative position to the frontier cells and the frontier's size. We tested our approach's performance on both heterogeneous and homogeneous groups of mobile robots in different environments. We measure both coverage performance and swarm formation statistics that permit the group to maintain communication. Through a series of comparison experiments, we demonstrate the proposed strategy has superior performance over recently presented map coverage methodologies and the conventional artificial potential field based on a percentage of cell-coverage, turnaround, and safe paths while maintaining a formation that permits short-range communication.

**Index Terms**—Robot Flocking Systems, Heterogeneous Swarm, Area Coverage Algorithm, Obstacle Avoidance Algorithm, Distributed Control Architecture

## I. INTRODUCTION

Exploration and area coverage are two of the most challenging problems for systemic coordination of multiple agents, where they are required to maintain situational awareness within unknown arbitrary environments. Solving these problems can benefit many potential applications including environmental waste management [1], patrolling [2], search and rescue [3], and medicine therapy using nanobots [4].

The concepts of exploration and area coverage in robotics describe two different problems that serve distinct objectives. Unlike the exploration problem's objectives, which are mainly for identifying the structure of un-visited areas and map construction, the area coverage task aims at visiting or periodically re-visiting all necessary locations within a particular place for a purpose such as lawn mowing, painting or reconnaissance [5].

Single-agent space coverage [6, 7] has been dealt by many researchers. Single agents may be the best approach when assets are expensive and sufficient time is available e.g. planetary exploration missions. However, navigating and exploring

The authors are with the School of Engineering and Information Technology, University of New South Wales, Canberra, Australia. The Commonwealth of Australia supported this research through a Defence Science Partnerships agreement with the Australian Defence Science and Technology Group.

a wide area with a single robot suffers from drawbacks, including long turnaround time, depletion of robot power sources, and poor quality and quantity of information collected [8]. In particular, single agents are not an ideal selection for surveillance or disaster response when mission time is critical.

In a modern multi-agent coverage system, information about the explored space is shared with nearby agents. Each agent maintains its own map and performs its own space coverage strategy. Most popular approaches still rely upon centralized control, and hence, distributed decision making is ignored [9, 10]. However, as centralised control greatly depends on high-bandwidth reliable communications, its performance degrades significantly in new and unidentified environments, where communication bandwidth is limited or intermittent and especially when the number of agents increase. Multi-agent coverage is widely considered in a distributed fashion [8, 11-13]. Operating a distributed robotics framework substantially reduces the load of communication and enhances the resilience and competence of system connectivity - important factors for large-scale networks [14]. Another upside of the distributed system is that agents can have lower computational requirements and can consequently be of lower cost and more easily replaced [15].

Furthermore, a common assumption in the recent works related to distributed multi-robot systems [16-19], is the availability of a known environment to model or powerful processors onboard each robot to perform the computational complexity. In unknown or large-scale environments, whose characteristics are complicated, their coverage performance can dramatically degrade.

Additionally, many related algorithms, for example, graph-based approaches [20] and Voronoi-based approaches [21], performed covering with the individual robot behaviors [17], which is independent of each other. The failure of a single robot can cause incomplete area coverage. Thus, robot cooperation is requisite to obtain fast and accurate map coverage. Motivated by emergent behaviors of animal aggregation found in insects, birds, fish, and other organisms, the interdisciplinary fields of swarm intelligence and robotics takes advantage of complex yet efficient and safe self-organized swarm formations by building a system of apparently simple interaction rules that take local observable information and limited-range communication among proximate agents as inputs [22].

Different from the Vicsek model [23], where flocking is generated by the combination of only self-propulsion and effective alignment, Reynolds model [24] easily incorporates the collective behavior and swarming with other operations, such as reaching the goal and avoiding obstacles. Noticeably,

although robots know their absolute locations at each time step, the Reynolds model-based flocking methods do not require highly accurate positioning, which is the main drawback of several formation control strategies. They decompose the complicated group behaviors to three simple steering rules (e.g., cohesion, alignment, or separation) at the individual agent level while the nearby agents move within the relevant radius, improving the robustness of the multi-agent swarm system [25]. Nevertheless, most of the existing studies have merely focused on formation control systems for the multi-robot area coverage applications. As such, the Reynolds model have not been rigorously discussed.

Furthermore, most recent relevant algorithms employing Reynolds model only operate with homogeneous groups of mobile robots [26-28] and perfect communication channels. This paper presents algorithms as applied to both homogeneous and heterogeneous robot swarms in various unknown environments with limited-range communications.

While most of the coverage strategies have just focused on obstacle-free environments [9, 16-18, 29], the real-world generally contains obstacles, such as humans, trees, or buildings, and hence there is a necessity for an integrated obstacle avoidance law. Due to the apparent simplicity and efficiency for real-time swarm robot applications, several efforts associated with the artificial potential field (APF) techniques have been explored to avoid unexpected collisions with obstacles. Many relevant examples can be found in [30, 31]. Nonetheless, the robots applying the APF law often get trapped in local minima or demonstrate path oscillations [32]. Deep reinforcement learning obstacles avoidance (DRLOA) systems have also been developed to deal with complex obstacle avoidance circumstances; however, a long pre-training process with expert demonstrations have been required [33].

Many current map exploration techniques are based on the definition of a *frontier*, which is the border between unexplored and known open areas. However, its application for area coverage has not yet been investigated. The space to be covered is divided into cells, and solving the coverage problem means discovering each cell by a robot at least once. Hence, the proposed research in this paper aims to develop a unified and distributed frontier-based coverage approach, along with a novel obstacle avoidance approach, which will be able to work in unknown environments using different types of bio-inspired swarm mobile robots.

In summary, our specific contributions, addressing current research challenges, can be emphasized as follows:

- 1) A novel, distributed algorithm leveraging the strengths of frontier-based area coverage and swarm behaviors, called frontier-led swarming (FS), is introduced, with a new and efficient obstacle avoidance algorithm based on Lidar information. Compared to several recently published coverage strategies, this algorithm allows the robotic swarms to achieve faster coverage, maintain better communication and stay away from local minima traps caused by interaction with obstacles.
- 2) Each agent can directly exchange the individual coverage and obstacle information with a set of neighbors without passing through a central station. Thus, the system is

distributed and the loss of a subset of agents does not critically affect the operation of the remaining swarm members in completing the overall mission.

- 3) System robustness and fault tolerance of the proposed strategy is validated and analysed through a series of real experiments.
- 4) This paper also performs a rigorous comparative study. The results of our space coverage algorithm are benchmarked against the frontier-based map coverage strategy without swarming, and three different map coverage algorithms. The algorithms are tested on both homogeneous and heterogeneous robot teams to cover a map as quickly as possible while maintaining a close self-organized swarm formation to permit short-range communication.

The rest of this paper is organized as follows. In Section 2, a literature review of related papers is presented. The problem formulation and the preliminaries are pointed out in Section 3. The architecture of the coverage algorithm and the obstacle avoidance strategy are introduced in Section 4. Experimental environment and the results are discussed in Section 5. Finally, some concluding remarks are presented in Section 6.

## II. RELATED WORK

This section reviews some research literature associated with the two key challenges in area coverage problems, the viewpoint generation and the path generation [8].

### A. Viewpoint Generation

Viewpoint generation describes the production of waypoints and poses of a vehicle during coverage. Viewpoint generation is an essential aspect of an area coverage problem because it provides the necessary guidance for the planning of the coverage path or behaviour of the agents so that they can cover the structure or environment of interest as fast as possible.

Several previous studies propose **model-based** viewpoint generation approaches. The work in [34, 35] decomposed an area of interest into sub-regions and then assigned sub-regions to different robots. Many recent studies [16-18] propose a new solution for minimum time coverage using a group of unmanned vehicles. The coverage problem is considered as a vehicle routing problem. In this method, the area of interest is decomposed into a set of sweeping line rows, as depicted in Fig. 1. The number of sweeps corresponds to the number of robots required for the coverage accomplishment.

Although model-based techniques are quite useful, they possess great computational complexity. In addition, these approaches are more suitable if one has a prior model of the environment, especially if there are complex shapes. In the cases of unobserved or large scale environments, whose characteristics are difficult to determine, model-less viewpoints generation techniques are preferred.

Frontier-based methods are a range of state-of-the-art **model-less techniques** aimed at leveraging the great benefits of tree-based frameworks and search algorithms, which are reported to dominate recent literature on environment exploration and map construction tasks due to their accuracy

and efficiency [36-38]. The desirable unexplored sub-areas searched by a tree-based algorithm, so-called frontiers, are assigned as temporary destinations to visit by a single or a group of robots. When there are no new frontiers left to detect, the entire environment is deemed to have been explored thoroughly [5]. Some other techniques based on frontiers that reduce the computational requirements and exploration turnaround can be found in [39-41]. It is to be noted that the frontier-based exploration can perform well not only on a single mobile platform but also on multiple robots [42, 43].

Our study proposes a partially model-based method that leverages the frontier search algorithm's advantages to control the swarm coverage behaviors. Our approach includes a model-based component that only requires the environment's size as prior knowledge to form a spatial coverage matrix within each individual robot's memory. The matrices' coverage status is shared locally to shape the swarm behaviors, leading to efficient exploration and coverage. In the multi-agent coverage problem, we assume there is no prior knowledge of the obstacles located in the unknown landmarks. Thus, a fully model-based method is inapplicable as it is impossible to compute a trajectory beforehand. Here, a frontier-based (model-less) component is introduced to guide each robot to novel areas while obstacle avoidance behavior is achieved using a dynamic repulsive force technique.

### B. Path Generation

In a noteworthy work introduced by Wang, Liang, and Guan [44], the frontier search algorithm was combined with particle swarm optimization (PSO) to improve the coverage capability of a swarm of mobile robots. The algorithm implements two working states: exploration and walking. In the exploration state, robots in a networked team discover their own non-overlapping sub-regions by travelling to local frontiers within such sub-areas. Once a robot explores all cells in its assigned area, it adapts a walking state to find another sub-area to explore using the PSO algorithm. The PSO algorithm aggregates three behaviours: a force representing the robot's direction in the previous time step, an attraction force toward the closest frontier cell in the map, and a force vector toward a frontier cell whose location is pointed to by the least number of other robots' movement vectors. When it reaches another sub-area, the exploration state starts again. This algorithm encourages the swarm dispersion to cover more space within a period, which might lead to inefficient communication and insufficient knowledge sharing among swarm members as the environment scales up.

Cheng et al. [45] implement a dynamic area coverage algorithm utilizing a swarm of autonomous robots, along with a leader-follower formation strategy. The robots possess only limited-range sensing and data processing capabilities. Due to these limitations, the authors present a hypothesis which states that using a flocking approach to create a formation of robots during the task would improve the exploration and coverage effectiveness and efficiency. The follower robots' location in the formation is dynamically adapted based on the movement of a leader robot in order to avoid obstacles. Meanwhile, a

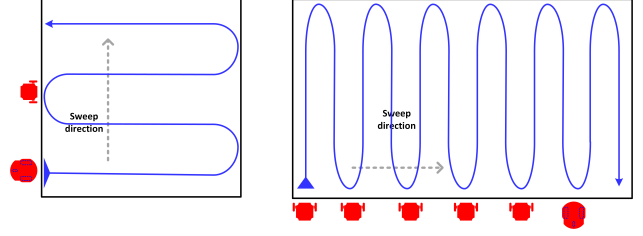


Fig. 1: Routing-based coverage strategy. A rectangular field is covered using a back-and-forth motion along routes perpendicular to the sweep direction and turns along borders.

Braitenberg-motion-based coverage strategy is applied to cover the environment. Their findings demonstrate that the formation of multiple robots created by flocking behaviors is superior to an individual coverage strategy in terms of completion time and stability.

As described earlier in this section, for the area coverage problem, the cooperative robots need to discover unknown environments in minimum time, maintain proximity to support communication and improve robustness and flexibility through distributed decision making. The research in this paper is motivated by these goals.

### III. PROBLEM FORMULATION AND PRELIMINARIES

To define the coverage problem a grid discretisation of a space is generally first defined with a certain resolution. Grids can be of different shapes including cells with triangular, square, hexagonal or diamonds shapes [8]. Different definitions of coverage of the grid exist, including dynamic coverage and static coverage [46]. In **static coverage**, agents need to seek out optimal locations that form an appropriate geometry so that their network of sensors can cover the whole environment [47]. However, in some practical missions, the environment cannot be fully covered by a static coverage geometric network due to the limitation in sensing range as well as the lack of mobile agents. In such cases, the problem of **dynamic coverage** is considered, where each mobile robot with limited-range sensors continuously moves and samples data, normally from unit spaces within a discretized domain until a predefined coverage level is attained [48]. In this paper, we focus on the dynamic coverage problem in unknown obstacle environments using a robotic swarm.

In a simple formal definition of dynamic coverage, a 2D grid cell  $j$  is covered by agent  $A^i$  if  $A^i$  was within cell  $j$  at some point during the exploration [49]. In that case, we say that  $A^i$  has **directly covered** cell  $j$ .

In a multi-agent system, if agent  $A^i$  communicates the coverage of cell  $j$  to a neighbour agent  $A^k$ , we say that agent  $A^k$  has **indirectly covered** cell  $j$ . **Synchronised coverage** is achieved in a multi-agent system when each agent has directly or indirectly covered all grid cells of the map. In other words, each agent knows that each cell has been directly covered by a certain agent.

#### A. Reynolds' Boids Model of Swarming

A basic boids swarming model [24] can be viewed as a type of rule-based reasoning to create swarming. The three

fundamental rules are:

- Cohesion: An agent should move towards the average position of its neighbours.
- Alignment: An agent should steer to align itself with the average heading of its neighbours.
- Separation: An agent should move to avoid collision with its neighbours.

The rules are generally implemented as forces that act on agents when a certain condition holds. Suppose we have a group of  $N$  agents  $A^1, A^2, A^3 \dots A^N$ . At time  $t$ , agent  $A^i$  has a position,  $p_t^i$ , and a flocking velocity,  $v_{flock(t)}^i$ . At each time step  $t$ , the velocity of agent  $A^i$  is updated as follows:

$$v_{flock(t+1)}^i = v_{flock(t)}^i + W_c v_{c(t)}^i + W_a v_{a(t)}^i + W_s v_{s(t)}^i + (W_{av} v_{av(t)}^i) \text{ or } (W_w v_{w(t)}^i) \quad (1)$$

$v_{c(t)}^i$  is the vector of cohesion force;  $v_{a(t)}^i$  is the vector of alignment force;  $v_{s(t)}^i$  is the vector of separation force;  $v_{w(t)}^i$  is the vector of wall avoidance force; and  $v_{av(t)}^i$  is the vector of obstacle avoidance force. Different positive weights  $W_c$ ,  $W_a$ ,  $W_s$ ,  $W_w$ , and  $W_{av}$ , are used to characterize the strengths of corresponding forces. Once a new velocity has been computed, the position of  $p_{t+1}^i$  of agent  $A^i$  in the next time step  $t+1$  is computed as follows:

$$p_{t+1}^i = p_t^i + v_{flock(t+1)}^i \quad (2)$$

Formally, we can define a subset  $\mathcal{N}^i$  of agents within a certain range  $R$  of  $A^i$  as follows:

$$\mathcal{N}^i = \{A^k \mid k \neq i \wedge \|p_t^k - p_t^i\|_2 < R\} \quad (3)$$

The number of agents in such a subset can be denoted by  $|\mathcal{N}^i|$ . Different ranges may be used to calculate cohesion, alignment and separation forces respectively, or other factors such as the communication range of a boid. The average position  $\bar{c}_t^i$  of agents in subset  $(\mathcal{N}_c)_t^i$  whose positions are within the cohesion range  $R_c$  of  $A^i$  is calculated as:

$$\bar{c}_t^i = (\sum_k p_t^k) / |\mathcal{N}_c_t^i| \quad (4)$$

The vector of cohesion force is the vector from the current position of agent  $A^i$  towards this average position:

$$v_{c(t)}^i = \bar{c}_t^i - p_t^i \quad (5)$$

Similarly, we can calculate the average position  $\bar{s}_t^i$  of agents in subset  $(\mathcal{N}_s)_t^i$  whose positions are within the separation range  $R_s$  of  $A^i$  as:

$$\bar{s}_t^i = (\sum_k p_t^k) / |\mathcal{N}_s_t^i| \quad (6)$$

The vector away from this position is calculated as:

$$v_{s(t)}^i = p_t^i - \bar{s}_t^i \quad (7)$$

The average velocity  $v_{a(t)}^i$  of agents in subset  $(\mathcal{N}_a)_t^i$  whose positions are within the alignment range  $R_a$  of  $A^i$ , is calculated by:

$$v_{a(t)}^i = (\sum_k v_{flock(t)}^k) / |\mathcal{N}_a_t^i| \quad (8)$$

These vectors can then be normalised and multiplied with their corresponding weights, before calculating the next velocity. The newly calculated velocity may be further normalised

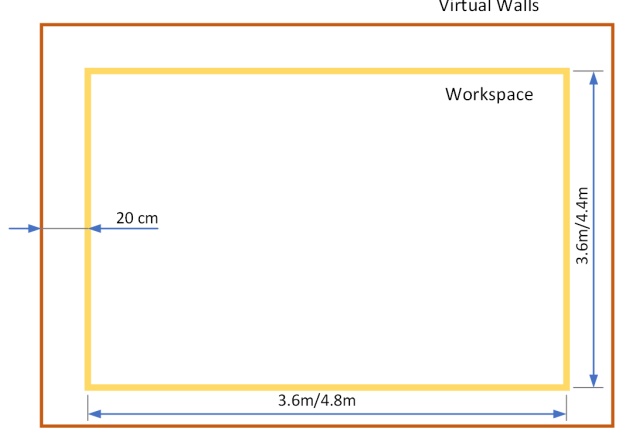


Fig. 2: Virtual wall avoidance approach.

and then scaled by a speed value chosen between a range of  $[V_{min}, V_{max}]$ .

Since the physical VICON environment is not bounded by any real walls, the LiDar sensor cannot measure the relative distance information with the boundaries. For simplicity, a wall collision avoidance velocity has been designed to keep the robots within a rectangular workspace. The wall collision avoidance velocity  $v_{w(t)}^i$  is defined by two components for a 2-D environment:

$$w_{x(t)}^i = \begin{cases} -1 & \text{if } x_t^i < \underline{x} \\ 0 & \text{if } \underline{x} \leq x_t^i \leq \bar{x} \\ 1 & \text{if } x_t^i > \bar{x} \end{cases} \quad (9)$$

$$w_{y(t)}^i = \begin{cases} -1 & \text{if } y_t^i < \underline{y} \\ 0 & \text{if } \underline{y} \leq y_t^i \leq \bar{y} \\ 1 & \text{if } y_t^i > \bar{y} \end{cases} \quad (10)$$

$$v_{w(t)}^i = (w_{x(t)}^i, w_{y(t)}^i), \quad (11)$$

where  $(\underline{x}, \bar{x})$  and  $(\underline{y}, \bar{y})$  denote the left, right, bottom, and top limits of the workspace.

The virtual wall is described as in Fig. 2. There is one offset (0.2 m) between the workspace and the virtual walls. The robot, therefore, does not hit the virtual wall and miss any cell located at the edge of the workspace.

However, in an unknown complex urban-like environment, the proposed virtual wall avoidance strategy is replaced by the obstacle avoidance strategy. Similar to the force calculation formula against walls, the virtual obstacle avoidance force contributed by obstacles, which is defined to be inversely proportional to the relative position between the  $i^{th}$  robot and the unexpected obstacle  $p_{ro}^i$ , can be computed as follows when the collision distance  $R_{av}$  is violated:

$$v_{av(t)}^i = \begin{cases} -p_{ro(t)}^i & \text{if } p_{ro(t)}^i \leq R_{av} \\ 0 & \text{if } p_{ro(t)}^i > R_{av} \end{cases} \quad (12)$$

#### IV. ARCHITECTURE OF THE PROPOSED COVERAGE METHOD

The primary research purpose is to design a distributed area coverage controller with a dynamic capability to tackle a cluttered environment. Therefore, this section is split into four relevant parts: space coverage matrix, frontier search algorithm, and the proposed controller design.

##### A. Shared Coverage and Obstacle (CO) Matrix

Unlike a centralized setting where a global common coverage matrix is used by all agents, every agent in a distributed setting stores, in its own memory, a 2D array  $C_{A^i}$  composed of square grid cells of value  $\varphi_{A^i}(X, Y)$  of appropriate resolution  $\varepsilon$  covering the environment whose maximum and minimum coordinates  $\bar{\cdot}$  and  $\underline{\cdot}$  on the  $x$  and  $y$  axes are given. The map can be decomposed into dimensions as follows:

$$\dim(X, Y) = \text{int}((\bar{x} - \underline{x}, \bar{y} - \underline{y})/\varepsilon) \quad (13)$$

where  $x$  and  $y$  are positive integer numbers. For each agent, all cells are first initialised as uncovered:

$$\varphi_{A^i}(X, Y) = 0, \quad \forall X, Y \in \mathbb{N}. \quad (14)$$

If the agent passes through an undiscovered or covered square cell  $(X, Y)$ , then set:

$$\varphi_{A^i}(X, Y) = 1. \quad (15)$$

Otherwise, if the agent senses an obstacle cell  $(X, Y)$  within an obstacle detecting radius, then set:

$$\varphi_{A^i}(X, Y) = 2. \quad (16)$$

When the distance between two agents  $A^i$  and  $A^k$  are smaller than  $R_c$ , they will exchange the local CO grids together. Agent  $A^i$  will update its internal grid with agent  $A^k$ 's grid map to produce a new CO grid in the next time step:

$$\varphi_{A^i}(X, Y)(t+1) = \max(\varphi_{A^i}(X, Y)(t), \varphi_{A^k}(X, Y)(t)). \quad (17)$$

By only using short-range communications, the network load is reduced and the swarm is more robust to range limitations such as loss of line-of-sight. Short-range agent communications are more effective when swarming rules are applied since the robots regularly move close together due to the attraction forces. As the swarming behaviour creates more inter-robot interactions and sharing of data, the turnaround time can also be reduced.

##### B. Frontier Search

In frontier search, the environment is approximated into a 2D or 3D grid map, where each cell possesses an occupancy value of 1 for explored, or 0 for unexplored, respectively. The frontier is defined as a segment that separates explored cells from unexplored cells. Therefore, any undiscovered spots, which are adjacent to at least one free cell (or unoccupied cell), are grouped into frontier regions. The descriptions expressed above are depicted in Fig. 3.

Let  $n_t^j$  denote the frontier node  $j$  at time step  $t$ . First, all valid frontier nodes at time  $t$  are collected into a list of frontier nodes  $\Gamma_t = [n_t^0, \dots, n_t^J]$ , arranged in a queue data structure as described by Algorithm 1. A breadth-first search (BFS) algorithm, illustrated in Algorithm 2, is then implemented on each frontier node in  $\Gamma_t$  to map the frontier cells and relevant unexplored cells into a corresponding frontier region and add it in a set  $\Xi_t = \{\zeta_t^1, \dots, \zeta_t^H\}$ ,  $H \leq J$ . Each frontier region is comprised of its frontier and the unexplored cells within its boundary. Finally, the frontier regions are ranked based on minimising the Euclidean distance from the closest frontier node of that region to the robot's current position  $D_t^{j \rightarrow \zeta_t^h}$  and the grid size of the frontier area that frontier node represents  $S_t^{j \rightarrow \zeta_t^h}$ . The utility function is defined as below:

$$F_{\zeta_t^h} = \Psi_D D_t^{j \rightarrow \zeta_t^h} - \Psi_S S_t^{j \rightarrow \zeta_t^h}, \quad (18)$$

$$\tilde{\zeta}_t = \arg \min_{\zeta_t^h \in \Xi_t} F_{\zeta_t^h}, \quad (19)$$

where  $\Psi_D$  and  $\Psi_S$  represent weighting parameters associated with the two terms. It can be seen that Eq. 18 is minimized when the distance is small and the frontier size is large.

After an accessible frontier  $\tilde{\zeta}_t$  is determined as a desired destination by (19), the algorithm then steers the robot towards that region's centroid. The searching process is repeated in each robot member until no more frontiers in the internal maps are found.

---

##### Algorithm 1 Frontier node search

---

**Input:** current cell  $c_t(X, Y)$

**Output:** list of frontiers  $\Xi_t$

Initialize a queue with  $c_t(X, Y)$  as element  $\Omega \leftarrow c_t(X, Y)$   
 Initialize a list of frontiers  $\Xi_t \leftarrow \emptyset$   
**while**  $\Omega$  is **not** empty **do**  
 Pop a cell  $c \in \Omega$   
 Get set  $\Pi$  including 4-connected cells of  $c$   
**for**  $c' \in \Pi$  **do**  
**if**  $c'$  is a free cell **then**  
 Add to queue  $\Omega \leftarrow c'$   
**end if**  
**if**  $c'$  is an unexplored frontier cell **and**  $c'$  does not belong to any frontier **then**  
 Find frontier region  $\zeta_t(c')$  using Algorithm 2  
 Add to frontier list  $\Xi_t \leftarrow \zeta_t(c')$   
**end if**  
**end for**  
**end while**  
**Return**  $\Xi_t$

---

##### C. Frontier-Led Swarming

After the best frontier cell is selected, the attractive velocity toward the centre of the chosen frontier  $p_{\tilde{\zeta}}$  acting on the relevant robot is obtained by:

$$v_{frontier} = \begin{cases} p_{\tilde{\zeta}} - p^r, & \text{if } v_s^r = 0 \\ 0, & \text{if } v_s^r \neq 0 \end{cases}, \quad (20)$$

**Algorithm 2** Frontier region connectivity search

**Input:** frontier cell  $n_t^j$ 
**Output:** a frontier region contains frontier and unexplored cells as 8-connected region  $\zeta_t(n_t^j)$ 

 Initialize a queue with  $n_t^j$  as element  $\Phi \leftarrow n_t^j$ 

 Initialize frontier region  $\zeta_t(n_t^j) \leftarrow n_t^j$ 
**while**  $\Phi$  is not empty **do**

 Pop a cell  $c \in \Phi$ 

 Get set  $\Pi$  including 8-connected cells to  $c$ 
**for**  $c' \in \Pi$  **do**
**if**  $c'$  is an unexplored free cell **then**

 Add to queue  $\Omega \leftarrow c'$ 

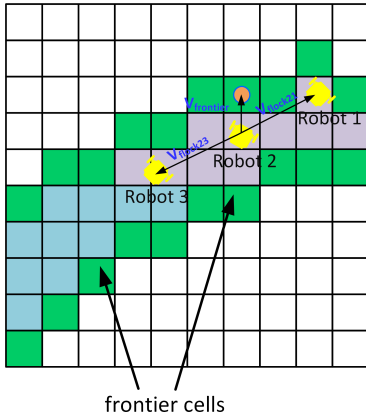
 Add to frontier region  $\zeta_t(n_t^j) \leftarrow c'$ 
**end if**
**end for**
**end while**
**Return**  $\zeta_t(n_t^j)$ 


Fig. 3: Fused velocity of the robot 2.

In case the same best cell is simultaneously selected by the two robots, a potential robot-robot collision can occur. To solve this issue, when two robots are closer than the critical circle radius  $R_s$ , they compute only the separation vector and neglect the frontier vector, as indicated in (20).

The fused velocity vector, as shown in Fig. 3, is the summation of the frontier velocity and the flocking velocities:

$$v_r = \sum_{i=1}^N v_{flock}^i + v_{frontier}. \quad (21)$$

Based on the fused velocity vector, the robot's linear and angular velocity can be computed as follows:

$$V = \sqrt{v_{rx}^2 + v_{ry}^2} \quad (22)$$

$$\omega = k(\text{atan}2(v_{ry}, v_{rx}) - \theta),$$

where  $(v_{rx}, v_{ry})$  indicate the robot velocities on the  $x$  and  $y$  axes.  $\omega$  is the robot's angular velocity. Furthermore,  $\theta$  is the robot's heading angle and  $k$  is a constant gain.

Fig. 4 illustrates a flowchart of the whole proposed control algorithm while Table I shows all the major parameters set

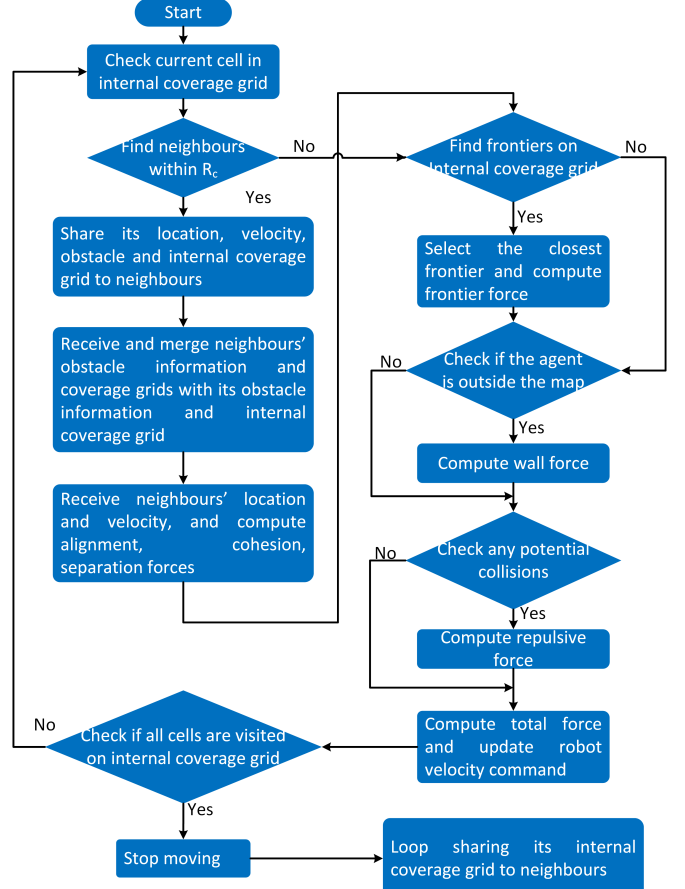


Fig. 4: Flow chart of the proposed control algorithm.

up for the physical experiments, for the two different types of robots employed in this work.

TABLE I: TurtleBot Burger and Pioneer 3-DX Robot Parameters

Parameter	Description	Burger	P3-DX
$W_a$	Alignment Weight	0.5	0.6
$W_c$	Cohesion Weight	0.23	0.21
$W_s$	Separation Weight	1.1	1.2
$W_w$	Wall Weight	1.1	0.05
$W_f$	Attractive force Weight	0.08	0.03
$W_{av}$	Avoiding force Weight	1.1	1.1
$\Psi_1$	Frontier Distance Weight	0.001	0.001
$\Psi_2$	Frontier Size Weight	1.0	1.0
$R_a$ (m)	Alignment Radius	1.5	1.5
$R_s$ (m)	Separation Radius	0.65	0.85
$R_c$ (m)	Cohesion Radius	1.5	1.5
$R_{av}$ (m)	Avoiding Radius	1.7	1.7
$\bar{V}$ (m.s <sup>-1</sup> )	Maximum linear speed	0.25	0.25
$\bar{\theta}$ (o.s <sup>-1</sup> )	Maximum angular speed	0.9	0.9

TABLE II: Environment Parameters

Parameter	Description	Values
$\varepsilon$	Coverage Matrix Resolution	0.3 m

## D. Obstacle Avoidance Strategy

In an uncertain or unknown environment, the robot can collide with another robot or an unexpected obstacle when

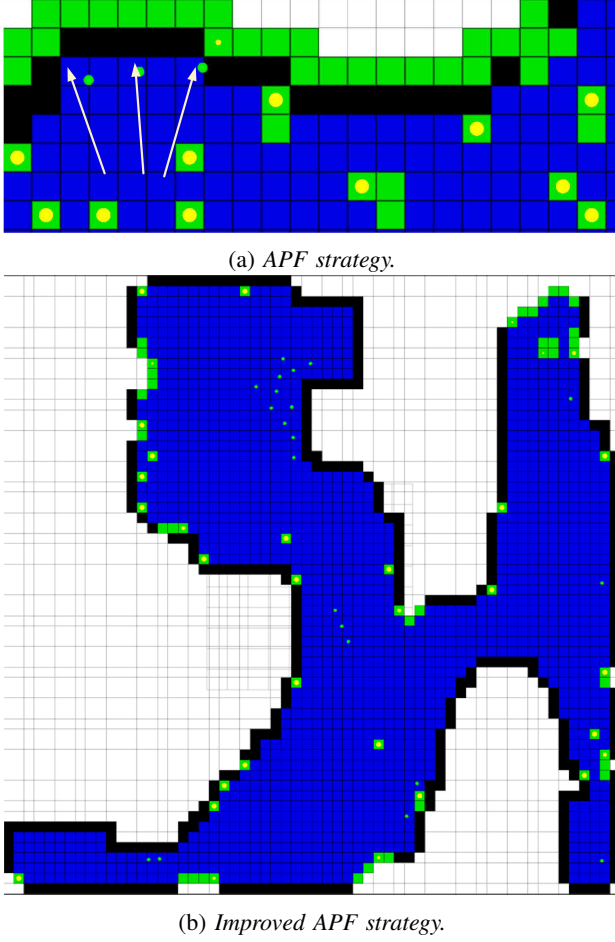


Fig. 5: Obstacle avoidance capability of the proposed obstacle avoidance technique with respect to the conventional APF.

traveling to the target point without a proper obstacle avoidance strategy. LiDar sensor provides data to implement a suitable obstacle avoidance algorithm. Instead of implementing the distance-based virtual repulsive force calculation as in (12), a dynamic distance-based repulsive scale  $\delta$  is employed in this work to steadily convert the cohesion and alignment velocity vectors into the collision avoidance force as in (23)-(26). By doing this, the attractive force and the repulsive force acting on the robot will not be cancelled out when the robot is exploring near obstacle clutters or in narrow passages (within  $R_{av}$ ) (see Fig. 5).

$$\delta_{(t)}^i = \frac{R_{av} - p_{ro(t)}^i}{R_c} \quad (23)$$

$$W_{av}^{i'} = W_{av}^i \delta_{(t)}^i \quad (24)$$

$$W_a^{i'} = W_a^i \max((1 - 2\delta_{(t)}^i), 0) \quad (25)$$

$$W_c^{i'} = W_c^i \max((1 - 2\delta_{(t)}^i), 0) \quad (26)$$

## V. EXPERIMENTAL RESULTS AND DISCUSSION

In this section, the performance of the Frontier-Led Swarm (FS) algorithm is examined and compared with four alternatives. The first is the proposed Frontier (F) algorithm without

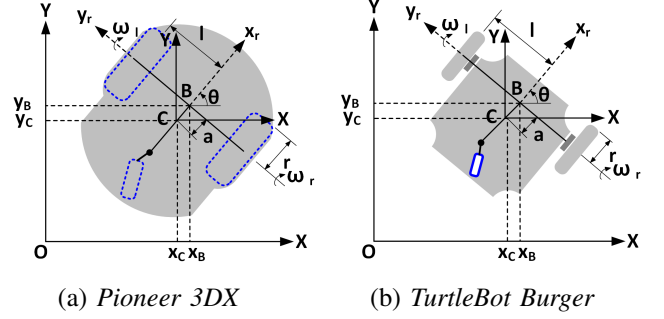


Fig. 6: Schematic of two autonomous ground vehicles.

**swarming**. This approach uses the frontier force and separation rule only (to prevent robots colliding). The second is a basic (non-frontier) spatial coverage method with swarming (BS). This approach uses the same collective intelligence of robotic swarms and shared coverage matrix. However, instead of using a frontier attraction force  $v_{frontier}$ , the final velocity is computed with an attractive force toward an unexplored cell searched by Algorithm 3 [49]. The third is swarming (S) only without any frontier or other attractive component towards unexplored cells [50]. Finally, multi-vehicle routing-based area coverage approaches [17, 18] are also considered in the comparative experiments.

**Algorithm 3** Cell selection of the basic space coverage approach

**Input:** current cell  $c_t^0$ ; list of unexplored cells  $\Theta_{u(t)}$ ; the map size; and the coverage matrix resolution  $\varepsilon$

**Output:** Closest unexplored cell  $c_{u(t)}^*$

Initialize the dimensions of coverage matrix by Equation 13. Convert the robot position from the global coordinate frame into the coverage map coordinate frame.

**for**  $c_{u(t)}^j \in \Theta_{u(t)}$  **do**

    Find distance to all unexplored cells:

$$d_t^j = \|c_t^0 - c_{u(t)}^j\|_2$$

**end for**

Select the closest unexplored cell:

$$c_{u(t)}^* = \operatorname{argmin}_{c_{u(t)}^j \in \Theta_{u(t)}} (d_t^j)$$

**Return**  $c_{u(t)}^*$

## A. Experimental Setup

The experiments in this paper use TurtleBot Burger and Pioneer 3DX robots. These are small, reliable, low-cost two-wheel differential unmanned ground vehicle (UGV) platforms (see Fig. 6). The robots are controlled by on-board computers integrated with the Robot Operating System (ROS) and other compatible open-source software, and utilise sensors including 360-degree LiDAR.

To control these UGVs, ROS supports two control input signals, namely yaw rate and linear velocity. These desired speeds are computed using Eq. 22, and then used as the

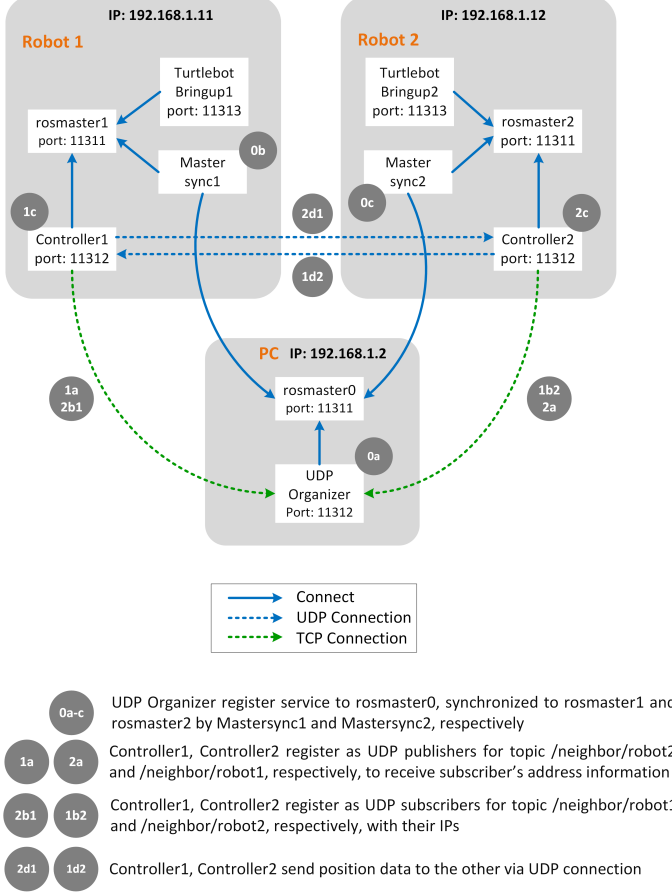


Fig. 7: Distributed *Multi-ROS Master* architecture for the swarming behavior of the cooperative ground vehicles. Only two robots shown for simplicity.

reference signals for inner loop PID controllers which control the servo motors driving the wheels of each robot type.

In the real-time experiments, the behavior of all robots is captured by a VICON Tracker motion capture system and transmitted to each robot every 0.02s through the User Datagram Protocol (UDP) network protocol. In real applications, this central localisation node is no longer used as a real GPS or ultra-wideband (UWB) sensor mounted on each robot provides the global robot position. The individual coverage matrices for each robot are shared among the neighbouring robots at an update rate of 0.01s. The sampling time is fixed at 0.02s. To improve the robustness of the map coverage task, all proposed methods and the multi-ROS Masters were implemented on each robot (see Fig. 7). If one of the robots fails due to power outages or hardware problems, the remaining robots can still complete the task. Hence, compared to other coverage techniques running a single ROS Master [51, 52], our control architecture is more reliable and robust. In simulations, the same settings are implemented using ROS and Gazebo tools.

The overall evaluation metrics for the different algorithms presented in this article are the coverage percentage ( $CP$ ) (27), the turnaround time ( $TT$ ), and two metrics for analyzing swarm behaviours. The first metric for swarm behaviours is the 'group' metric  $G$  (28), which estimates 'how' closely clustered together a set of the robots is (a lower value indicates greater

grouping). The second metric for swarming is the 'order' metric  $O$  (29), which computes 'how well' aligned the robots are (a lower value indicates greater alignment). **Five tests** were conducted for each **experiment**, and the evaluation metrics' **mean and standard deviation** are computed and shown in all tables.

$$CP = \frac{|\Theta_e|}{|\Theta|} 100\% \quad (27)$$

where  $|\Theta_e|$  and  $|\Theta|$  are the number of covered cells and the total number of cells to be covered in this problem respectively.

The grouping metric  $G$  is defined by Equation 28 where  $N_r$  is the number of the cooperative robots,  $\bar{p}_r$  is the average position of the  $N_r$  robots at the given time, and  $T_0$  is the time that the robots start swarming (within  $R_c$ ).

$$G = \sum_{t=T_0}^{T_0+15dt} \frac{\frac{1}{N_r} \sum_{i=1}^{N_r} \|p_r^i - \bar{p}_r\|_2}{N_G}, \quad (28)$$

where  $dt$  depicts the sample time.  $N_G = 15$  represents the sample length of the group metrics.

Likewise the order metric  $O$  is defined by Equation 29 below where  $\bar{v}_r$  is the average velocity of the  $N_r$  robots at the given time.

$$O = \sum_{t=T_0}^{T_0+15dt} \frac{\frac{1}{N_r} \sum_{i=1}^{N_r} \|v_r^i - \bar{v}_r\|_2}{N_O}, \quad (29)$$

Here,  $N_O = 15$  represents the sample length of the order metrics.

Two experimental environments were established: (1) a small, empty square arena ( $3.6 \times 3.6$ m) and (2) a larger ( $4.4 \times 4.8$ m) square arena with four boxes utilized as obstacles. The static obstacles in the big map (Fig. 8) are represented by the black square objects. The physical robotic agents, denoted as green circles, have two different types: homogeneous (seven TurtleBots) and heterogeneous (six TurtleBots and two Pioneers), as shown in Fig. 9. The frontier region, the unexplored cells, the explored cells, and the chosen frontier cell are represented by green square cells, white square cells, blue square cells, and yellow circle cells, respectively.

For measurement purposes in this paper, we assume that once all frontier cells in the local map are covered directly or indirectly, the robot is stopped at the final target, and a message 'completed task' is sent to the remaining robots and, if applicable, a base station or operator through a separate low-bandwidth longer range link. This message may also contain the complete coverage map, or the robot may be programmed to return to a set location to update other robots or the base station/operator with the final map. In our case we simply allow the other robots to continue their individual missions until each has its own complete coverage map.

All video demonstrations showing a spatial coverage distribution of Robot 1 under the control of all solutions can be viewed at the following address: [https://youtu.be/4mDpP\\_TMjFU](https://youtu.be/4mDpP_TMjFU); <https://youtu.be/XqiMdQJvkjQ>; [https://youtu.be/2t-X7\\_5FeIY](https://youtu.be/2t-X7_5FeIY); and <https://youtu.be/xOJvz0ee0sg>.

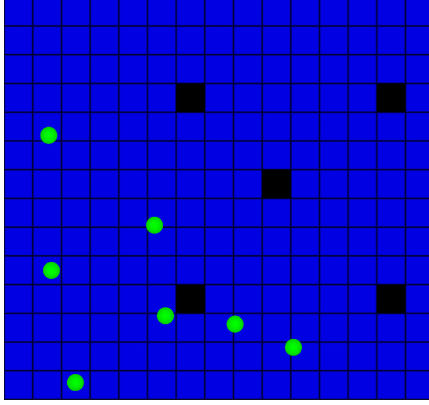


Fig. 8: Large map region and obstacles. Green spheres describe the robot positions while blue squares depict the covered cells. Further, black squares are the obstacle cells.



Fig. 9: Six Turtlebot and two Pioneer UGVs demonstrating the collective behavior and spatial coverage.

#### B. Experiment 1: Frontier-Led Swarming (FS) versus Frontier (F), Basic Swarm (BS) and Swarm (S) Algorithms

Tables III-IV and the video demos present the coverage performances in multi-agent coverage problems. Both frontier strategies are able to cover the whole region with satisfactory performance ( $CPs = 100\%$ ). By traveling independently to the desired frontier cells, but less the inter-robot communications, the FS approach exhibits quite similar  $TT$  figures as the F approach for both homogeneous and heterogeneous robot teams. Still, we can see that the proposed FS strategy is potentially suitable for a variety of system types, large numbers of cooperative robot networks, and coverage area as there are no mutual collisions recorded between the robot-robot and robot-obstacle objects.

On the other hand, the group metric indicates that FS is maintaining a closer formation than the F approach in all evaluation schemes. According to the 95% confident metrics, the difference is statistically significant. However, the FS formation is not as tight as for the S or BS approaches. This is likely due to the influence of the frontier rules pulling the swarm apart a little. The order metric is greater for the F approach than for FS, BS, and S. The difference is statistically significant in both cases. This makes sense because the swarming approaches should encourage ordering. All of these conclusions demonstrate the appropriate parameter configurations for all tests.

TABLE III: Experimental results of the various controllers for small area coverage.

Metrics	<b>Homogeneous Robots</b>	
	<b>FS</b>	<b>F</b>
<b>CP (%)</b>	$100.00 \pm 0.00$	$100.00 \pm 0.00$
<b>TT (s)</b>	$130.40 \pm 17.81$	$124.60 \pm 5.41$
<b>G (m)</b>	$1.00 \pm 0.00$	$1.37 \pm 0.01$
<b>O (m.s<sup>-1</sup>)</b>	$0.30 \pm 0.05$	$0.39 \pm 0.10$
Metrics	<b>BS</b>	
	<b>S</b>	
<b>CP (%)</b>	$100.00 \pm 0.00$	$100.00 \pm 0.00$
<b>TT (s)</b>	$143.40 \pm 26.54$	$142.00 \pm 18.02$
<b>G (m)</b>	$0.90 \pm 0.00$	$0.86 \pm 0.004$
<b>O (m.s<sup>-1</sup>)</b>	$0.31 \pm 0.08$	$0.29 \pm 0.10$
<b>Heterogeneous Robots</b>		
Metrics	<b>FS</b>	
	<b>F</b>	
<b>CP (%)</b>	$100.00 \pm 0.00$	$100.00 \pm 0.00$
<b>TT (s)</b>	$153.60 \pm 25.29$	$153.80 \pm 36.21$
<b>G (m)</b>	$1.09 \pm 0.00$	$1.29 \pm 0.01$
<b>O (m.s<sup>-1</sup>)</b>	$0.12 \pm 0.03$	$0.19 \pm 0.20$
Metrics	<b>BS</b>	
	<b>S</b>	
<b>CP (%)</b>	$100.00 \pm 0.00$	$100.00 \pm 0.00$
<b>TT (s)</b>	$153.82 \pm 22.38$	$179.17 \pm 23.16$
<b>G (m)</b>	$0.86 \pm 0.01$	$0.90 \pm 0.00$
<b>O (m.s<sup>-1</sup>)</b>	$0.11 \pm 0.07$	$0.12 \pm 0.01$

TABLE IV: Swarm results of the different coverage control approaches for large area coverage.

Metrics	<b>Homogeneous Robots</b>	
	<b>FS</b>	<b>F</b>
<b>CP (%)</b>	$100.00 \pm 0.00$	$100.00 \pm 0.00$
<b>TT (s)</b>	$233.20 \pm 25.00$	$239.4 \pm 41.45$
<b>G (m)</b>	$1.05 \pm 0.006$	$1.23 \pm 0.00$
<b>O (m.s<sup>-1</sup>)</b>	$0.12 \pm 0.00$	$0.16 \pm 0.08$
Metrics	<b>BS</b>	
	<b>S</b>	
<b>CP (%)</b>	$100.00 \pm 0.00$	$100.00 \pm 0.00$
<b>TT (s)</b>	$273.70 \pm 44.50$	$428.6 \pm 72.04$
<b>G (m)</b>	$0.94 \pm 0.00$	$0.88 \pm 0.01$
<b>O (m.s<sup>-1</sup>)</b>	$0.10 \pm 0.00$	$0.07 \pm 0.00$
<b>Heterogeneous Robots</b>		
Metrics	<b>FS</b>	
	<b>F</b>	
<b>CP (%)</b>	$100.00 \pm 0.00$	$100.00 \pm 0.00$
<b>TT (s)</b>	$222.6 \pm 14.30$	$213.60 \pm 11.80$
<b>G (m)</b>	$1.07 \pm 0.00$	$1.28 \pm 0.00$
<b>O</b>	$0.12 \pm 0.02$	$0.15 \pm 0.01$
Metrics	<b>BS</b>	
	<b>S</b>	
<b>CP (%)</b>	$100.00 \pm 0.00$	$100.00 \pm 0.00$
<b>TT (s)</b>	$240.20 \pm 38.02$	$331.40 \pm 55.16$
<b>G (m)</b>	$0.93 \pm 0.00$	$0.91 \pm 0.00$
<b>O (m.s<sup>-1</sup>)</b>	$0.11 \pm 0.01$	$0.10 \pm 0.01$

Moreover, from the FS group and order metric rows in the two tables, we can observe that the robots'  $G$  clustering locations with respect to the average robot positions are within  $R_c$  (1m and 1.49m) and the velocity differences  $O$  among robots maintain low values in all cases ( $0.3m.s^{-1}$  and  $0.11m.s^{-1}$ ). This validates the swarming quality of the presented method.

According to the results in Tables III and IV, the swarm metrics  $G$  and  $O$  yield desirably small values, meaning that the quality of swarming in both cases is still satisfactory and similar. However, the FS controller performing flocking behaviors and coverage is able to explore the complex target environment noticeably faster than the BS and S controllers. The better-unexplored cell selection approach is the main difference between the FS control strategy and other conven-

TABLE V: Experimental evaluation of the three controllers for large area coverage.

Metrics	Heterogeneous Robots		
	FS	Routing	RandRouting
CP (%)	100.0 $\pm$ 0.0	100.0 $\pm$ 0.0	100.0 $\pm$ 0.0
TT (s)	227.3 $\pm$ 30.0	308 $\pm$ 32.2	142.0 $\pm$ 5.4

tional methods. This is reflected in the  $TT$  numbers. The BS completes the spatial coverage task at approximately 273s for a homogeneous system and 240s for a heterogeneous system. These results are greater than the coverage performance of FS by 40s and 18s, respectively. Finally, although the S coverage method achieves the best swarm behavior, it completely covers the large spaces in the slowest turnaround, namely 331.4s, as each unexplored cell is only reached by chance.

### C. Experiment 2: Frontier-led Swarming versus Multi-Robot Routing

The next experiment is used to explore the performance of the multi-vehicle routing approach to our FS strategy. This comparative approach is evaluated in two cases: the pre-defined starting robot positions (Routing) and randomly starting robot positions (RandRouting).

The large and free space of the environment is fit into seven sweeps, and hence the seven mobile robots are applied to carry out the coverage task. As can be seen in Fig. 10, all of these strategies achieve complete coverage. Particularly, all  $CP$  rows in Table V are 100%. Additionally, compared to the two remaining coverage approaches, the Routing approach performs coverage in the shortest time, approximately 142s, since the robots only track their own trajectory, and the flocking behaviors and separation forces do not impact them. However, this algorithm is not robust and implemented in a partially distributed fashion, where each robot is tasked to cover a sub-area and track the pre-defined trajectory. Therefore, the individual robot failure during execution can jeopardize the completion of the area coverage task. Moreover, it also requires prior knowledge of the structure or environment, resulting in a low autonomous ability. Finally, this method can only be applied to clear regions with no obstacles.

The enhanced coverage algorithm RandRouting is a more promising path-planning solution for the distributed multi-robot coverage problem. Nevertheless, the cooperative robots under the RandRouting approach spend 308s to complete the full area coverage, which is slowest among the three strategies. Some new cells along the desired trajectory can be missed due to drift movements, sharp turns, and inter-robot collision avoidance. These cells can only be revisited when the robots implement the backtracking paths. Hence, as specified in Table V and the swarm metrics, our presented coverage method obtains a reasonable turnaround and better system stability.

### D. Experiment 3: Robustness of Frontier-Led Swarming

In the third experiment, during the coverage mission, two robots among a team of eight heterogeneous mobile robots are randomly either shut down or turned on after every

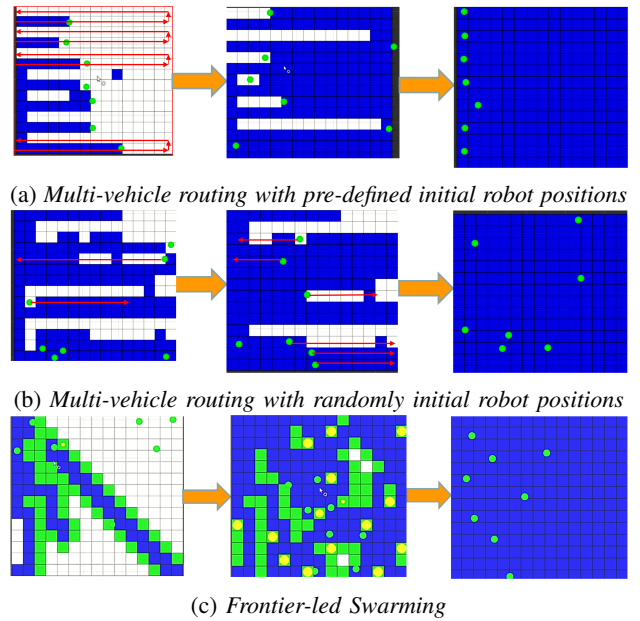


Fig. 10: Cooperative robot area coverage of the three comparative controllers, including the Routing, PPBSCR and FS.

30s. Furthermore, the inter-robot communications are used to validate the health status of each robot. Suppose the neighbor data has been interrupted. After an interval of 3s, the associated robot is considered ‘lost,’ and the cohesion and alignment forces acting on the remaining robots will be removed. Separation forces continue to be applied based on LiDAR range information provided from the still active robots. This prevents the lost robot becoming a collision hazard to the other swarm members. However, if the failed robot’s neighbor data is recovered, it can immediately continue the area coverage task with the default settings.

Fig. 11 describes graphically the map coverage processing of heterogeneous multi-robot systems using the collective behaviors and frontier-based coverage. Thanks to the distributed and multi-ROS Master architecture, the whole area is still fully covered (ie.  $CP = 100 \%$ ). Moreover, although two of the robots are deactivated every 30s, the coverage completion time  $TT$  is reasonably low, namely,  $372 \pm 24.76$  s. Compared to the centralized or partially distributed path planning-based coverage algorithms [17, 18], where individual robot failures (the robot is not capable of operating and moving anymore) can cause the breakdown of the whole task or damage to other robots, our proposed strategy is superior.

Furthermore, the robustness of the proposed coverage algorithm is examined in a cluttered environment, where the imperfect LiDar and VICON measurement data (measurement noise level is approximately 0.1m) causes the mismarking of a black obstacle cell and the blue coverage cells. As depicted in the plots of Fig. 12, the obstacle cells have been corrected to the coverage cells right after the robots bypass those cells (no obstacle is detected, and hence, no obstacle avoidance force is applied). Additionally, if the position error is less than or equal to a cell resolution, the coverage performance of the frontier method is still satisfactory as the coverage error is

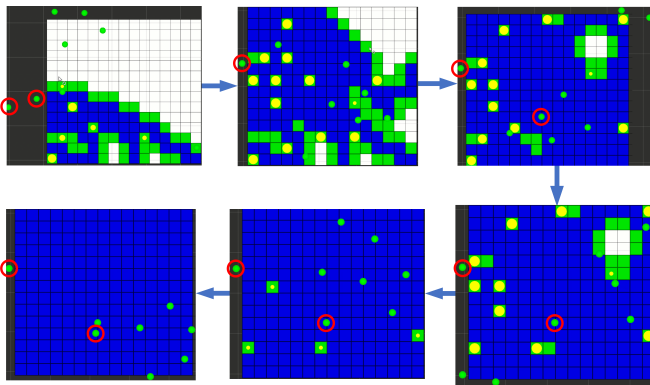


Fig. 11: Heterogeneous UGVs are flocking, exploring, and covering a new area over time. The two failed ground vehicles are marked with red circles.

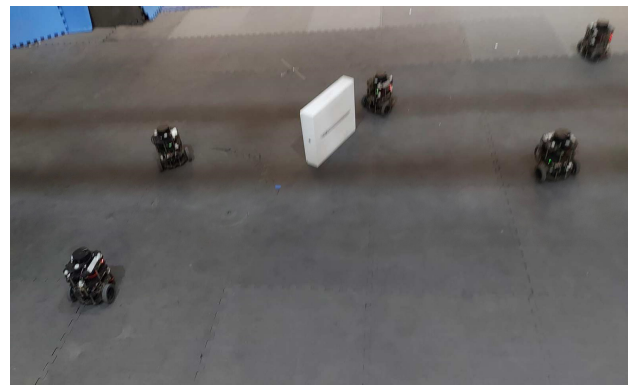
either only 0 cell (large resolution) or 1 cell (small resolution). More importantly, the desired performances of obstacle avoidance and flocking behavior are also guaranteed in the presence of LiDAR measurement disturbance, where there is no obstacle-robot or robot-robot collisions recorded, and  $G$  and  $O$  metrics remain within reasonable bounds of  $1.05 \pm 0.078$ m and  $0.15 \pm 0.015$ m, respectively. Consequently, all frontier cells in Robot 1's internal map have been covered, and the coverage task has been accomplished after only 220.6s. Accordingly, the proposed strategy can handle various uncertainties, which is far superior to many recent SLAM approaches demanding accurate global navigation, such as GMapping [53].

#### E. Experiment 4: FS Algorithm for a Simulated Complex Environment

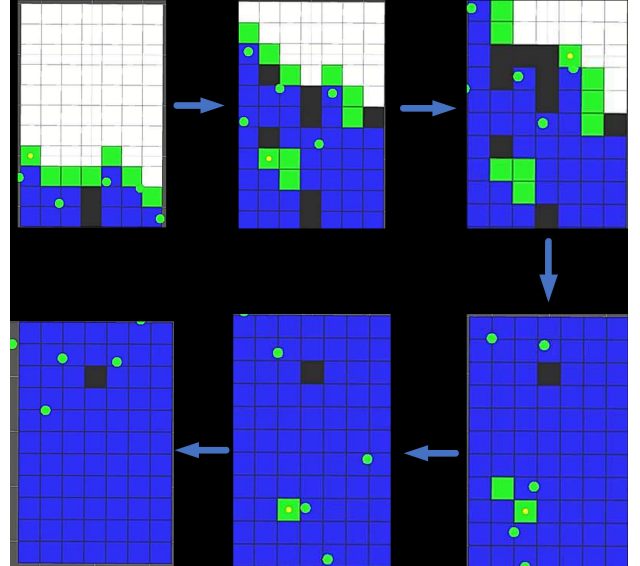
Since our real-world VICON space is limited, a 2D large-scale urban-like scenario ( $120mL \times 90mW$ ) cluttered with obstacles, and a large-scale heterogeneous multi-robot system (sixteen Turtlebot Burger3 and seven Pioneer 3DX ground vehicles) are constructed and simulated in a virtual Gazebo world to test the performance of all mentioned comparative methods (see Fig. 13).

The experiment was repeated 5 times for each designed method and the configuration settings are identical to those used in the physical experiments (Table I), except that the cell resolution  $\varepsilon$  is increased to 1m. Besides coverage information exchange, the obstacle location is sensed by LiDAR sensors on each robot and shared among a group of neighbouring robots. At the beginning of the experiment, the robot locations are pre-defined.

All coverage, obstacle avoidance, and collective behaviors in simulations are the same as those implemented in online tests. As summarised in Table VI, our proposed FS technique enables the robots to cover the whole unknown region with the smallest turnaround (1522.3s of the FS approach compared to 1773.3s, 2234s, and 2325.7s of the F, BS, and S approaches, respectively, in the equivalent scenario) when safely overcoming the building blocks and guaranteeing the swarm formation in close vicinity. Comparing the results of the FS with the results of the F, the turnaround is considerably shorter and the final average coverage rate is higher as the covered cell



(a) Real workspace with one obstacle.



(b) Collective behavior and frontier-based coverage observed in RViz interface.

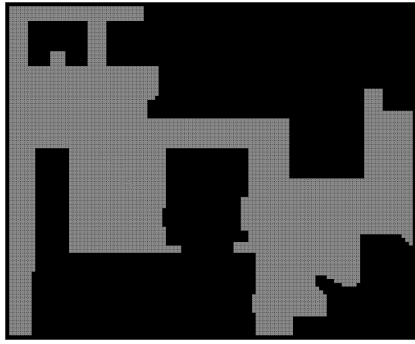
Fig. 12: Coverage Performance in a cluttered environment.

information is shared among the UGVs more times due to the collective behaviors, especially in huge spaces. Furthermore, the space coverage task cannot be accomplished by the BS approach in a favorable coverage period as only 96% of cells are explored within 2325.7s. Two key reasons lead to this negative result. Firstly, it is observed that the attractive force and the repulsive force acting on each robot are often canceled out when the robot is navigating between two facing obstacles. This can cause the robot to be stationary for an extended period. Secondly, the cell selection method is not optimal. The conclusions consolidate our arguments that the frontier-driven swarming algorithm with obstacle avoidance is also well-suited for various undiscovered and cluttered environments.

Finally, Table VII summarises the turnaround time measured with respect to various values of the robot quantities and urban-like environmental scale. Each result is computed by averaging over ten different trials. Firstly, the more robots are involved in the coverage experiment; the quicker turnaround can be obtained. However, if the number of robots reaches saturation, the completion time may increase slightly. For example, the 80 robots case takes 45s more than the 70 robots



(a) Real built environment.



(b) Virtual Gazebo environment.

Fig. 13: Unknown complex urban-like environment.

TABLE VI: Evaluation metrics of the different methodologies for urban area coverage.

Metrics	<i>Heterogeneous Robots</i>	
	<i>FS</i>	<i>F</i>
<i>CP (%)</i>	$100.00 \pm 0.00$	$98.00 \pm 0.62$
<i>TT (s)</i>	$1522.30 \pm 98.80$	$1773.30 \pm 166.90$
<i>O</i>	$0.34 \pm 0.01$	$0.39 \pm 0.00$
Metrics	<i>BS</i>	<i>S</i>
<i>CP (%)</i>	$96.00 \pm 5.00$	$95.00 \pm 3.68$
<i>TT (s)</i>	$2234.00 \pm 92.50$	$2325.70 \pm 43.80$
<i>O (m.s<sup>-1</sup>)</i>	$0.33 \pm 0.00$	$0.27 \pm 0.00$

case to entirely cover the same  $(40 \times 40)$ m arena. This makes sense as all robots in the former case must avoid mutual collisions more times. Noticeably, it is clear that the distributed frontier-led swarm control system can work well for the large-scale deployment of robots and maps.

TABLE VII: Turnaround time vs. Robot Numbers vs. Environmental Size

Environmental Size ( $m \times m$ )	No. of Robots	Turnaround Time (s)
$40 \times 40$	40	$467.25 \pm 62.88$
	50	$371.79 \pm 80.78$
	60	$327.60 \pm 74.70$
	70	$321.00 \pm 88.77$
	80	$366.88 \pm 58.28$
$80 \times 80$	40	$1002.42 \pm 171.04$
	50	$883.20 \pm 123.33$
	60	$816.81 \pm 161.42$
	70	$807.27 \pm 157.07$
	80	$725.58 \pm 155.82$

## VI. CONCLUSION

This paper developed a new biologically inspired approach to control autonomous multi-robot coordination, especially focusing on space coverage and surveillance for entirely unknown environments. The most significant features of the proposed approach are pointed out as follows:

- 1) **Adaptability:** the presented technique can be used in various environments.
- 2) **Flexibility:** the algorithm can perform appropriately with various types of robotic platforms (homogeneous and heterogeneous robots) without re-tuning many parameters.
- 3) **Scalability:** the Frontier-led swarm control system works for any number of robots and any coverage map size (time to coverage reduces when the number of robots increases).
- 4) **Robustness and fault tolerance:** due to the multi-ROS Master implementation and local communication, an individual robot's failure does not stop the whole system from functioning and completing the mission. Additionally, the frontier-led swarm algorithm, improves coverage behavior in cluttered environments.

The real-world and simulation comparisons reveal that the frontier-based multi-agent map coverage algorithm with swarming and obstacle avoiding behaviors, designed in the paper, outperforms most of the conventional space coverage systems (e.g., the BS and S in all given tests and F in the urban environment) and the conventional APF in terms of turnaround time, coverage percentage, and collision number. Moreover, compared to the traditional frontier-based exploration methods using a centralised node to assign frontiers, or the recent coverage protocols (e.g., Routing and RandRouting) which require prior knowledge of environments, our proposed techniques do not need a model of the environment. Besides, they are also fully distributed and robust to robot failures, disturbed and uncertain environments. As shown in videos and Fig. 4, each robot in a collaborative team implements the frontier-based coverage strategy on its local map and shares acquired local coverage information with only other active neighbours, resulting in a similar map with a matching set of frontiers. The inter-robot communication, therefore, is said to be short-ranged ( $R_c = 1.5$ m), which is suitable for swarm mobile robots application in cluttered environments.

However, the presented controller cannot track environmental changes (e.g., moving obstacle avoidance or new events) taking place in the explored cells and update the coverage map accordingly. For our future work, the proposed coverage method will be combined with a digital pheromone implementation to drive periodic revisit of cells to update and correct the coverage information based on a pheromone evaporation period.

## REFERENCES

- [1] C. P. Le, A. Q. Pham, H. M. La, and D. Feil-Seifer. A multi-robotic system for environmental dirt cleaning. In *2020 IEEE/SICE International Symposium on System Integration (SII)*, pages 1294–1299. IEEE, 2020.
- [2] T. Kuyucu, I. Tanev, and K. Shimohara. Superadditive effect of multi-robot coordination in the exploration of unknown environments via stigmergy. *Neurocomputing*, 148:83–90, 2015.

[3] K. Albina and S. G. Lee. Hybrid stochastic exploration using grey wolf optimizer and coordinated multi-robot exploration algorithms. *IEEE Access*, 7:14246–14255, 2019.

[4] A. Williams, B. Sebastian, and P. Ben-Tzvi. Review and analysis of search, extraction, evacuation, and medical field treatment robots. *Journal of Intelligent & Robotic Systems*, 96(3-4):401–418, 2019.

[5] Sujata Sharma and Ritu Tiwari. A survey on multi robots area exploration techniques and algorithms. In *2016 International Conference on Computational Techniques in Information and Communication Technologies (ICCTICT)*, pages 151–158. IEEE, 2016.

[6] M. Torres, D. A. Pelta, J. L. Verdegay, and J. C. Torres. Coverage path planning with unmanned aerial vehicles for 3d terrain reconstruction. *Expert Systems with Applications*, 55:441–451, 2016.

[7] H. Liu, J. Ma, and W. Huang. Sensor-based complete coverage path planning in dynamic environment for cleaning robot. *CAAI Transactions on Intelligence Technology*, 3(1):65–72, 2018.

[8] R. Almadhoun, T. Taha, L. Seneviratne, and et al. A survey on multi-robot coverage path planning for model reconstruction and mapping. *SN Appl. Sci. I*, 847, 2019.

[9] Y. Khaluf and P. Simoens. Collective sampling of environmental features under limited sampling budget. *Journal of Computational Science*, 31:95–110, 2019.

[10] M. Schranz, M. Umlauft, M. Sende, and W. Elmenreich. Swarm robotic behaviors and current applications. *Frontiers in Robotics and AI*, 7:36, 2020.

[11] C. Luo, S. X. Yang, X. Li, and M. Q. Meng. Neural-dynamics-driven complete area coverage navigation through cooperation of multiple mobile robots. *IEEE Transactions on Industrial Electronics*, 64(1):750–760, 2017.

[12] K. Albina and S. G. Lee. Hybrid stochastic exploration using grey wolf optimizer and coordinated multi-robot exploration algorithms. *IEEE Access*, 7:14246–14255, 2019.

[13] J. Song and S. Gupta. Care: Cooperative autonomy for resilience and efficiency of robot teams for complete coverage of unknown environments under robot failures. *Autonomous Robots*, 44(3):647–671, 2020.

[14] M. Li, K. Lu, H. Zhu, M. Chen, S. Mao, and B. Prabhakaran. Robot swarm communication networks: architectures, protocols, and applications. In *2008 Third International Conference on Communications and Networking in China*, pages 162–166. IEEE, 2008.

[15] E. Şahin. Swarm robotics: From sources of inspiration to domains of application. In *International workshop on swarm robotics*, pages 10–20. Springer, 2004.

[16] A. Xu, C. Viriyasuthee, and I. Rekleitis. Efficient complete coverage of a known arbitrary environment with applications to aerial operations. *Autonomous Robots*, 36(4):365–381, 2014.

[17] G. S. Avellar, G. A. Pereira, L. C. Pimenta, and P. Iscold. Multi-UAV routing for area coverage and remote sensing with minimum time. *Sensors*, 15(11):27783–27803, 2015.

[18] N. Karapetyan, K. Benson, C. McKinney, P. Taslakian, and I. Rekleitis. Efficient multi-robot coverage of a known environment. In *2017 IEEE/RSJ International Conference on Intelligent Robots and Systems (IROS)*, pages 1846–1852, 2017.

[19] J. Nauta, Y. Khaluf, and P. Simoens. Hybrid foraging in patchy environments using spatial memory. *Journal of the Royal Society Interface*, 17(166):20200026, 2020.

[20] J. M. Palacios-Gasós, D. Tardioli, E. Montijano, and C. Sagüés. Equitable persistent coverage of non-convex environments with graph-based planning. *The International Journal of Robotics Research*, 38(14):1674–1694, 2019.

[21] O. Arslan and D. E. Koditschek. Voronoi-based coverage control of heterogeneous disk-shaped robots. In *2016 IEEE International Conference on Robotics and Automation (ICRA)*, pages 4259–4266. IEEE, 2016.

[22] M. Brambilla, E. Ferrante, M. Birattari, and M. Dorigo. Swarm robotics: a review from the swarm engineering perspective. *Swarm Intelligence*, 7(1):1–41, 2013.

[23] T. Vicsek, A. Czirók, E. Ben-Jacob, I. Cohen, and O. Shochet. Novel type of phase transition in a system of self-driven particles. *Physical review letters*, 75(6):1226, 1995.

[24] C. W. Reynolds. Flocks, herds and schools: A distributed behavioral model. In *Proceedings of the 14th annual conference on Computer graphics and interactive techniques*, pages 25–34, 1987.

[25] M. M. Khan, K. Kasmarik, and M. Barlow. Autonomous detection of collective behaviours in swarms. *Swarm and Evolutionary Computation*, page 100715, 2020.

[26] João Paulo Lima Silva de Almeida, Renan Taizo Nakashima, Flávio Neves-Jr, and Lúcia Valéria Ramos de Arruda. Bio-inspired on-line path planner for cooperative exploration of unknown environment by a multi-robot system. *Robotics and Autonomous Systems*, 112:32–48, 2019.

[27] D. Yu, C. L. P. Chen, C. E. Ren, and S. Sui. Swarm control for self-organized system with fixed and switching topology. *IEEE Transactions on Cybernetics*, 2019.

[28] R. Konda, H. M. La, and J. Zhang. Decentralized function approximated q-learning in multi-robot systems for predator avoidance. *IEEE Robotics and Automation Letters*, 5(4):6342–6349, 2020.

[29] X. Zhou, H. Wang, and B. Ding. How many robots are enough: a multi-objective genetic algorithm for the single-objective time-limited complete coverage problem. In *2018 IEEE International Conference on Robotics and Automation (ICRA)*, pages 2380–2387. IEEE, 2018.

[30] S. M. H. Rostami, A. K. Sangaiah, J. Wang, and X. Liu. Obstacle avoidance of mobile robots using modified artificial potential field algorithm. *EURASIP Journal on Wireless Communications and Networking*, 2019(1):70, 2019.

[31] Q. Li, J. Yuan, B. Zhang, and H. Wang. Artificial potential field based robust adaptive control for spacecraft rendezvous and docking under motion constraint. *ISA transactions*, 95:173–184, 2019.

[32] K. Biswas and I. Kar. On reduction of oscillations in target tracking by artificial potential field method. In *2014 9th International Conference on Industrial and Information Systems (ICIIS)*, pages 1–6. IEEE, 2014.

[33] S. Van Havermaet, Y. Khaluf, and P. Simoens. No more hand-tuning rewards: Masked constrained policy optimization for safe reinforcement learning. In *AAMAS2021, the 20th International Conference on Autonomous Agents and Multiagent Systems*, pages 1344–1352, 2021.

[34] A. Gautam, J. K. Murthy, G. Kumar, S. P. A. Ram, B. Jha, and S. Mohan. Cluster, allocate, cover: An efficient approach for multi-robot coverage. In *2015 IEEE International Conference on Systems, Man, and Cybernetics*, pages 197–203. IEEE, 2015.

[35] Jalil Modares, Farshad Ghanei, Nicholas Mastronarde, and Karthik Dantu. Ub-anc planner: Energy efficient coverage path planning with multiple drones. In *2017 IEEE international conference on robotics and automation (ICRA)*, pages 6182–6189. IEEE, 2017.

[36] R. Almadhoun, T. Taha, L. Seneviratne, J. Dias, and G. Cai. A survey on inspecting structures using robotic systems. *International Journal of Advanced Robotic Systems*, 13(6):1729881416663664, 2016.

[37] W. Gao, M. Booker, A. Adiwahono, M. Yuan, J. Wang, and Y. W. Yun. An improved frontier-based approach for autonomous exploration. In *2018 15th International Conference on Control, Automation, Robotics and Vision (ICARCV)*, pages 292–297. IEEE, 2018.

[38] F. Niroui, K. Zhang, Z. Kashino, and G. Nejat. Deep reinforcement learning robot for search and rescue applications: Exploration in unknown cluttered environments. *IEEE Robotics and Automation Letters*, 4(2):610–617, 2019.

[39] J. A. Caley, N. R. Lawrence, and G. A. Hollinger. Deep learning of structured environments for robot search. *Autonomous Robots*, 43(7):1695–1714, 2019.

[40] I. Arvanitakis, K. Giannousakis, and A. Tzes. Mobile robot navigation in unknown environment based on exploration principles. In *2016 IEEE Conference on Control Applications (CCA)*, pages 493–498. IEEE, 2016.

[41] M. M. Almasri, A. M. Alajlan, and K. M. Elleithy. Trajectory planning and collision avoidance algorithm for mobile robotics system. *IEEE Sensors journal*, 16(12):5021–5028, 2016.

[42] T. Cieslewski, E. Kaufmann, and D. Scaramuzza. Rapid exploration with multi-rotors: A frontier selection method for high speed flight. In *2017 IEEE/RSJ International Conference on Intelligent Robots and Systems (IROS)*, pages 2135–2142. IEEE, 2017.

[43] M. Juliá, A. Gil, and O. Reinoso. A comparison of path planning strategies for autonomous exploration and mapping of unknown environments. *Autonomous Robots*, 33(4):427–444, 2012.

[44] Y. Wang, A. Liang, and H. Guan. Frontier-based multi-robot map exploration using particle swarm optimization. In *2011 IEEE Symposium on Swarm Intelligence*, pages 1–6, 2011.

[45] K. Cheng, Y. Wang, and P. Dasgupta. Distributed area coverage using robot flocks. In *2009 World Congress on Nature Biologically Inspired Computing (NaBIC)*, pages 678–683, 2009.

[46] Y. Kantaros, M. Thanou, and A. Tzes. Distributed coverage control for concave areas by a heterogeneous robot-swarm with visibility sensing constraints. *Automatica*, 53:195–207, 2015.

[47] M. Zhong and C. G. Cassandras. Distributed coverage control and data collection with mobile sensor networks. *IEEE Transactions on Automatic Control*, 56(10):2445–2455, 2011.

- [48] Y. Wang and I. I. Hussein. Awareness coverage control over large-scale domains with intermittent communications. *IEEE Transactions on Automatic Control*, 55(8):1850–1859, 2010.
- [49] M. Masár. A biologically inspired swarm robot coordination algorithm for exploration and surveillance. In *2013 IEEE 17th International Conference on Intelligent Engineering Systems (INES)*, pages 271–275, 2013.
- [50] C. Chibaya and S. Bangay. Flock inspired area coverage using wireless boid-like sensor agents. In *Tenth International Conference on Computer Modeling and Simulation (uksim 2008)*, pages 144–149. IEEE, 2008.
- [51] R. N. Darmanin and M. K. Bugeja. Autonomous exploration and mapping using a mobile robot running ROS. In *ICINCO (2)*, pages 208–215, 2016.
- [52] Z. Li, Y. Xiong, and L. Zhou. ROS-based indoor autonomous exploration and navigation wheelchair. In *2017 10th International Symposium on Computational Intelligence and Design (ISCID)*, volume 2, pages 132–135. IEEE, 2017.
- [53] W. A. S. Norzam, H. F. Hawari, and K. Kamarudin. Analysis of mobile robot indoor mapping using gmapping based slam with different parameter. In *IOP Conference Series: Materials Science and Engineering*, volume 705, page 012037. IOP Publishing, 2019.